IRJSE Science & Engineering *Int. Res. J. of Science & Engineering*, 2018; Special Issue A5 : 1-6
ISSN: 2322-0015
SJIF Impact Factor 4.11
UGC Approved Journal No. 63628
RESEARCH ARTICLE
OPEN ACCESS

# IR Spectral and Elastic Moduli study of $Ho^{+3}$ doped Co–Ni ferrites via Sol–gel auto combustion Method

**[1]Fugate DV. [2] Ganure Ketankumar A, [2]Dhale Laxaman A, [3]Kadam Ankush. B**

*[1] Department of Physics, Shivaji College, Omerga Dist: Osmanabad (M.S.) India
[2]Department of Chemistry, Shrikrishna Mahavidyalaya, Gunjoti, 413606, Dist: Osmanabad
[3]Department of Physics, Jawahar Arts Science & Commerce College, Anudur Tq.Tuljapur,Dist.Osmanabad–413603
[1]first.author@abc.edu, [2]second.author@abc.edu, [1]third.author@abc.edu
*Corresponding author: E-mail: drabkadam@gmail.com

**Manuscript Details**

Available online on http://www.irjse.in
ISSN: 2322-0015

**Editor: Dr. Arvind Chavhan**

**Cite this article as:**
Fugate DV, Ganure Ketankumar A, Dhale Laxaman A, Kadam Ankush. B. IR Spectral and Elastic Moduli study of $Ho^{+3}$ doped Co–Ni ferrites via Sol–gel auto combustion Method, Int. Res. Journal of Science & Engineering, 2018; Special Issue A5: 1-6.



## ABSTRACT

Sol-gel auto combustion method is a well-defined reacting mixture for the synthesis of nano structured and functional ferrite particles of controlled size and shape having the general chemical formula $Co_{0.6}Ni_{0.4}Fe_{2-x}Ho_xO_4$ (x = 0.000 to 0.100 in the step of 0.025). The Fourier Transform Infrared Spectra (FT–IR) of the Co–Ni ferrite system have been analyzed in the frequency range of 200–800 $cm^{-1}$. The high frequency absorption band '$\upsilon_1$' assigned to tetrahedral complex and low frequency absorption band '$\upsilon_2$' assigned to octahedral complex. The force constant, bond length and Debye temperature were determined by infrared spectra analysis. The force constant, lattice constant and pore fraction have been used to investigate the elastic moduli such as Young's Modulus, Bulk Modulus, Rigidity Modulus.

**Key words:** Sol–gel, Co–Ni ferrites, IR, Elasticity.

## INTRODUCTION

Nanoscience and Nanotechnology is the technology dealing with both single nanoobjects and materials, and devices based on them, and with processes that take place in the nanometer range. Ferrites are magnetic ceramics containing iron oxide as a major constituent in it. Ferrite chip inductors





Principal
Jawahar Arts, Science & Commerce College,
Andur Tal. Tuljapur Dist, Osmanabad

are one of the important components for the latest electronics products such as cellular phones, video cameras, notebook computers, hard and floppy drives [1] etc. Ferrites are chemical compounds, ceramic with iron (III) oxide $Fe_2O_3$ as their principal components [2]. The presence of nonmagnetic ions in these spinel ferrites is found to alter their magnetic and electronic properties. The addition of metal cations such as trivalent or tetravalent influences the electronic and magnetic properties of the ferrite system [3-9]. The structural parameters as well as magnetic properties can be tuned by tailoring the composition of the material [10]. Now a day ferrite is used in telephone exchange, computers, and control equipment.

Many biotechnological applications have been developed based on biogenic and synthetic magnetic micro- and nanoparticles [11]. Magnetic nanoparticles have been used to guide radionuclides to specific tissues. An approach has been developed to directly label a radioisotope with ferrite particles [12] in vivo liver tissue in rats. Therapeutic applications are feasible by further conjugation with other medicals. Magnetic nanoparticles can also be used in a variety of applications: modification, detection, isolation, and study of cells [13], and isolation of biologically active compounds [14], for instance.

Co-Ni ferrite materials have gained the interest of researchers due to their remarkable properties such as high resistivity, high permeability and comparatively low magnetic losses. Co-Ni ferrites with high permeability and a high Curie temperature have been widely studied for practical and microwave applications [15-16]. The rare-earth (RE) ions substituted ferrites are becoming the promising materials for advanced applications, and addition of small amounts of rare-earth ions to ferrite samples can produce a larger improvement in their magnetic and electrical as well as structural properties.

The $Ho^{+3}$ doped $Co_{0.6}Ni_{0.4}Fe_{2-x}Ho_xO_4$ (x = 0.000 to 0.100 in the step of 0.025) ferrites were synthesized by sol gel auto combustion method to study the structural properties and elastic properties of the system.

## METHODOLOGY

The nano crystalline $Ho^{+3}$ substituted Co-Ni ferrite having chemical composition $Co_{0.6}Ni_{0.4}Fe_{2-x}Ho_xO_4$ (x = 0.000 to 0.100 in the steps of 0.025). Synthesized by Sol-gel auto-combustion method. The Pure (99%) AR grade corresponding nitrates Cobalt Nitrate ($Co(NO_3)_2.3H_2O$), Nickel Nitrate ($Ni(NO_3)_2.6H_2O$), Holmium Nitrate ($Ho(NO_3)_3.5H_2O$), Ferric Nitrate ($Fe(NO_3)_3.9H_2O$) and citric acid ($C_6H_8O_7.H_2O$), were used to prepare. Reaction carried out in air atmosphere without protection of inert gases. The molar ratio of metal nitrates to citric acid was taken as 1:3. The metal nitrates were dissolved together in a minimum amount of double distilled water to get a clear solution. An aqueous solution of citric acid was mixed with metal nitrates solution, then ammonia solution was slowly added to adjust the pH ≈7. Then the solution was heated at 90 °C to transform into gel. When ignited at any point of the gel, the dried gel burnt in a self-propagating combustion manner until all gels were completely burnt out to form a fluffy loose powder. The auto-combustion was completed within a minute, yielding the brown-colored ashes termed as a precursor. The as prepared powder then annealed at 600 °C for 4 hrs.

## RESULTS AND DISCUSSIONS

### Infrared Spectral studies

The Typical IR spectra of the composition $Co_{0.6}Ni_{0.4}Fe_{2-x}Ho_xO_4$ (x = 0.000 to 0.100 in the steps of 0.025) (x = 0.075) as shown in Fig. 1. The spectra are recorded in the range from 200 to 800 $cm^{-1}$. The absorption band '$\nu_1$' around 600 $cm^{-1}$ and '$\nu_2$' around 350 $cm^{-1}$ are the characteristic bands of spinel ferrite and are assigned to the vibrations of the metal ion-oxygen complexes in the tetrahedral-A and octahedral-B sites, respectively [17]. The vibration frequencies $\nu_1$ and $\nu_2$, respectively, corresponding to A and B sites for the investigated ferrites are given in Table 1.

**Table 1 Lattice constant 'a', X ray density 'dx', Bond lengths (RA & RB), Absorption bands ($\nu_1$ and $\nu_2$)Force constant 'K' and Poisson's ratio 'σ' of $Co_{0.6}Ni_{0.4}Fe_{2-x}Ho_xO_4$ (x = 0.000, 0.025, 0.050. 0.075, 0.100).**

| Comp.x | 'a' (Å) | '$d_x$' (g/cm$^3$) | $\nu_1$ (cm$^{-1}$) | $\nu_2$ (cm$^{-1}$) | $R_A$ (Å) | $R_B$ (Å) | $K_0 \times 10^5$ (dyne/cm) | $K_t \times 10^5$ (dyne/cm) |
|---|---|---|---|---|---|---|---|---|
| **0.000** | 8.410 | 5.330 | 600.31 | 350.27 | 3.862 | 3.064 | 1.1912 | 2.0023 |
| **0.025** | 8.415 | 5.382 | 594.65 | 348.75 | 3.864 | 3.065 | 1.1245 | 1.9056 |
| **0.050** | 8.422 | 5.413 | 592.73 | 345.91 | 3.866 | 3.066 | 0.9865 | 1.6834 |
| **0.075** | 8.429 | 5.453 | 589.59 | 342.74 | 3.868 | 3.067 | 0.8723 | 1.5167 |
| **0.100** | 8.435 | 5.515 | 586.73 | 340.03 | 3.870 | 3.068 | 1.0454 | 1.7851 |

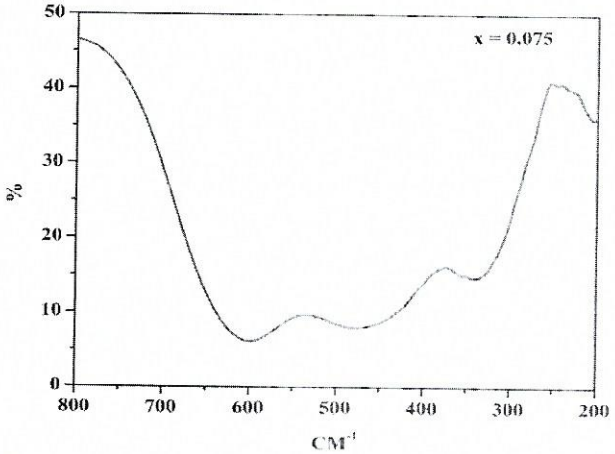


**Figure 1: The typical Infrared Spectrum of $Co_{0.6}Ni_{0.4}Fe_{2-x}Ho_xO_4$ (x = 0.075).**

The difference in band position is expected because of the difference in $Fe_B^{3+} - O_2^{2-}$ inter-ionic distance for the octahedral and tetrahedral coordination. The vibrational frequency depends on the cation mass, cation to oxygen distance and bonding force.

The force constant is second derivative of potential energy with respect to the site radius, the other independent parameters being kept constant. The force constant for tetrahedral site ($K_t$) and octahedral site ($K_0$) were calculated employing the method suggested by Waldron [17]. According to Waldron the force constant $K_t$ and $K_0$ for respective sites are given by

$$K_t = 7.62 \times M_1 \times \nu_1^2 \times 10^{-3} \quad (1)$$

$$K_o = 10.62 \times \frac{M_2}{2} \times \nu_2^2 \times 10^{-3} \quad (2)$$

Where, $M_1$ and $M_2$ are molecular weight of cations on A and B site respectively. The bond lengths $R_A$ and $R_B$ have been calculated using the formula Gorter [18].

The values of $R_A$, $R_B$ and force constant $K_t$ and $K_0$ are listed in Table 1.The bond lengths increase as $Ho^{+3}$ ions content increases and also the force constant $K_0$ decreased from $1.19\times10^5$ to $1.04\times10^5$ dyne/cm and $K_t$ decreased from $2\times10^5$ to $1.74\times10^5$ dyne/cm with the increase in substitution of $Ho^{+3}$ ions

**Elastic property Studies**

Elastic moduli and Debye temperature were calculated through IR data and structural data of the presently investigated spinel ferrite samples [19–21]. These elastic moduli were calculated using the values of lattice constant 'a', X-ray density 'dx', pore fraction 'f' and force constant 'K'.

The elastic constants are of much importance because they elucidate the nature of binding forces and to understand the thermal properties of solids. The elastic moduli often used are Young's modulus, Bulk modulus, Rigidity modulus and Poisson's ratio. Among all the elastic constants of ferrites, Young's modulus is special interest because it is the decisive factor for the most widely employed core shapes, namely rods and rings [19]. The stiffness constant ($C_{11}$) calculated using relation [22].

$$\text{Stiffness constant } (C_{11}) = \frac{K}{a} \quad (3)$$

$$\text{Stiffness constant } (C_{12}) = \frac{\sigma \quad C_{11}}{(1-\sigma)} \quad (4)$$

Where, K is average force constant; 'a' is lattice constant. The variation of stiffness constants decrease with increase in $Ho^{+3}$ ions content as shown in Figure 2.

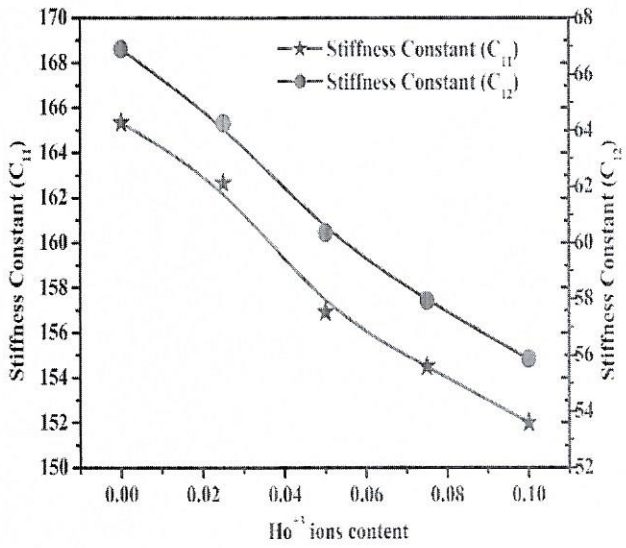


Figure 2

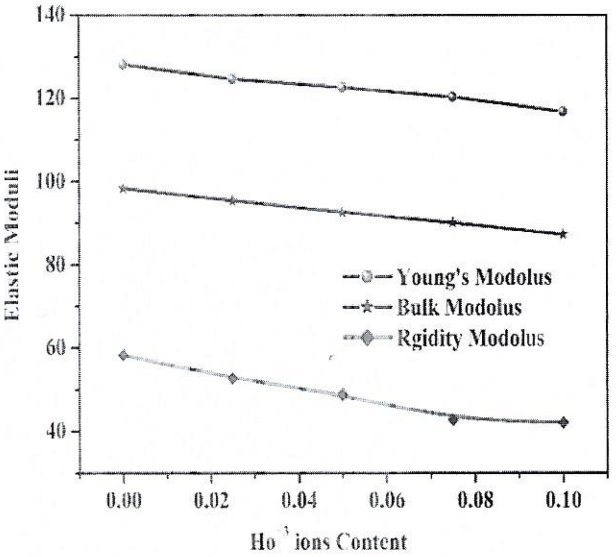


Figure 3

**Figure 2:** Variation of stiffness constant with $Ho^{+3}$ ions Content.
**Figure 3:** Variations of Elastic Moduli with $Ho^{+3}$ ions Content.

The other elastic moduli for cubic structure are calculated using following relation [23],

$$\text{Young's modulus (E)} = \frac{(C_{11}-C_{12})(C_{11}+2C_{12})}{(C_{11}+C_{12})} \quad (5)$$

$$\text{Bulk Modulus (K)} = \frac{1}{3}\left(C_{11}+C_{12}\right) \quad (6)$$

$$\text{Rigidity modulus } (G_O) = \frac{E}{2(\sigma+1)} \quad (7)$$

The Young's modulus (E), Bulk Modulus (K) and Rigidity modulus ($G_O$) calculated by using above equations. The elastic moduli decreases with increase in $Ho^{+3}$ ion content and variation of elastic moduli and $Ho^{+3}$ ion contents as shown in Figure 3.

The longitudinal elastic wave velocity ($V_L$) and transverse (Shear) wave velocity ($V_S$) was calculated using following equations,

$$\text{Longitudinal velocity } V_L = \left(\frac{C_{11}}{\rho}\right)^{1/2} \quad (8)$$

$$\text{Transverse (Shear) velocity } V_S = \left(\frac{G}{\rho}\right)^{1/2} \quad (9)$$

Where, G is rigidity modulus with correct zero pore fraction. The values of $V_L$ and $V_S$ used to calculate mean wave velocity ($V_m$) which used to calculate Debye temperature '$\theta_E$' calculated using formula;

$$\text{Debye temperature } (\theta_E) = \frac{h}{k}\left[\frac{3\rho q N_A}{4\Pi M}\right]^{1/3} \times V_m \quad (10)$$

Where, 'h' is planks constant, k is Boltzmann's constant, M is molecular weight, 'q' is a number of an atom in the unit formula and $V_m$ mean wave velocity.

$$\frac{3}{V_m^3} = \frac{1}{V_l^3} + \frac{2}{V_S^3} \quad (11)$$

The values of longitudinal velocity, shearing velocity and mean wave velocity are calculated using relation 8, 9 and 10 respectively.

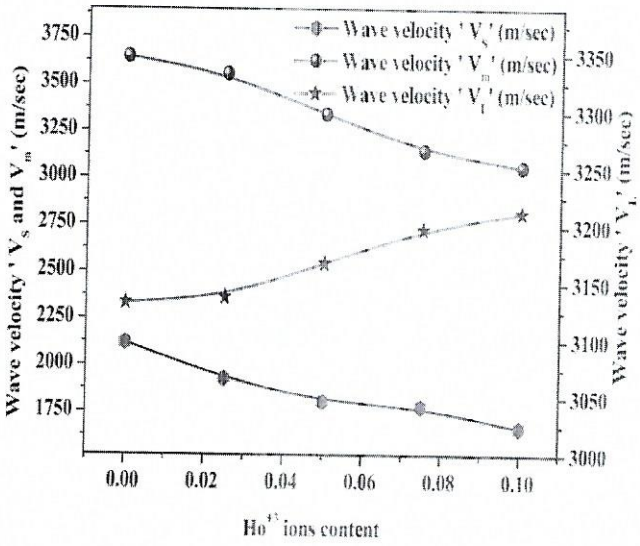


Figure 4

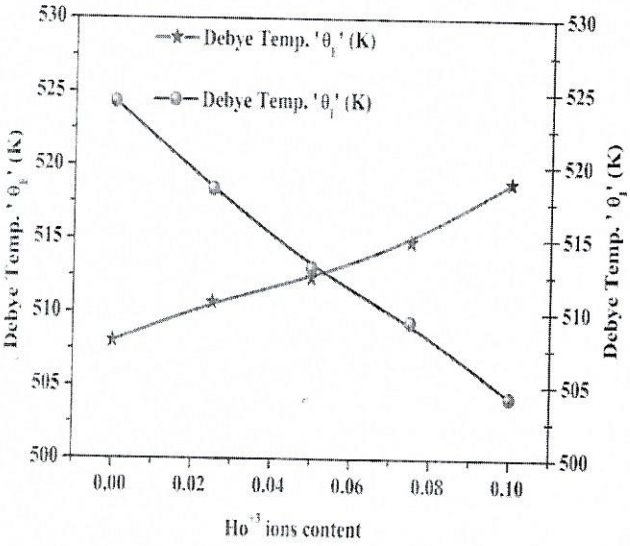


Figure 5

**Figure 4:** Variation of longitudinal wave velocity ($V_I$), shear wave velocity ($V_S$), *mean wave* velocity (Vm) with $Ho^{+3}$ ions Content.

**Figure 5:** Variation of Debye Temperature ($\theta_I$ and $\theta_E$) with $Ho^{+3}$ ions Content.

Figure 4 shows that the transverse (Shear) wave velocity ($V_S$) and mean wave velocity ($V_m$) decreases whereas the longitudinal elastic wave velocity ($V_L$) increased with $Ho^{+3}$ ions content. The values of wave velocities are similar to other ferrites those obtained from UPT method [24].

The Debye temperature increased with $Ho^{+3}$ ions content increase. The Debye temperature ($\theta_I$) obtained from IR data is compared with Debye temperature ($\theta_E$) the variation as shown in Figure 5.

## CONCLUSION

Sol-gel auto-combustion method to prepare the $Ho^{+3}$-doped nano ferro spinle compounds having the general formula $Co_{0.6}Ni_{0.4}Fe_{2-x}Ho_xO_4$ (x = 0.000 to 0.100 in the steps of 0.025). Infrared spectral shows two absorption bands '$\nu_1$' around 600 $cm^{-1}$ is assigned to the intrinsic stretching vibrations of tetrahedral complexes and band '$\nu_2$' around 350 $cm^{-1}$ is assigned as octahedral complexes. The bond lengths ($R_A$ and $R_B$) increases with increase in $Ho^{+3}$ ions content. Stiffness constants ($C_{11}$ and $C_{12}$) decreases with increase in $Ho^{+3}$ ions content. Variation of Elastic Moduli Young's modulus ($E$), Bulk modulus (K) and Rigidity modulus ($G$) decreases as $Ho^{+3}$ ions content increases. The variation of Debye temperatures ($\theta_E$ and $\theta_I$) is increases with $Ho^{+3}$ content and decrease in the rigidity of the ferrite.

## REFERENCES

1. Krishnaveni T, Kanth BR, Raju VSR & Murthy SR. Fabrication of multilayer chip inductors using Ni-Cu-Zn ferrites. *Journal of Alloys and Compounds*, *414*(1-2), 2006, 282-286.
2. Carter CB & Norton MG. *Ceramic materials: science and engineering*. Springer Science & Business Media,2007.
3. Lal R, Sharma ND, Taneja SP & Reddy VR. Structural and magnetic properties of zinc ferrite aluminates. *Ind. J. Pure and Appl. Phys.* 45,2007, 231.
4. Singhal S, Barthwal SK & Chandra K. Structural, magnetic and Mössbauer spectral studies of nanosize aluminum substituted nickel zinc ferrites. *Journal of magnetism and magnetic materials*, *296*(2), 2006, 94-103.
5. Pandit AA, Shitre AR, Shengule DR & Jadhav KM. Magnetic and dielectric properties of $Mg_{1+}$

$_xMn_xFe_{2-2x}O_4$ ferrite system. *Journal of materials science*, *40*(2), 2005, 423–428.

6. Singhal S, Singh J, Barthwal SK & Chandra K. Preparation and characterization of nanosize nickel-substituted cobalt ferrites ($Co_{1-x}Ni_xFe_2O_4$). *Journal of Solid State Chemistry*, *178*(10), 2005, 3183–3189.
7. Joseyphus RJ, Narayanasamy A, Shinoda K, Jeyadevan B & Tohji K. Synthesis and magnetic properties of the size-controlled Mn–Zn ferrite nanoparticles by oxidation method. *Journal of Physics and Chemistry of Solids*, *67*(7), 2006, 1510–1517.
8. Hastings JM & Corliss LM. Neutron diffraction study of manganese ferrite. *Physical Review*, *104*(2), 1956, 328.
9. Dhiman RL, Taneja SP & Reddy VR. Preparation and characterization of manganese ferrite aluminates. *Advances in Condensed Matter Physics*, *2008*.
10. Euliss LE, Grancharov SG, O'Brien S, Deming TJ, Stucky GD, Murray CB, & Held GA. Cooperative assembly of magnetic nanoparticles and block copolypeptides in aqueous media. *Nano Letters*, *3*(11), 2003, 1489–1493.
11. Xu C, Xu K, Gu H, Zhong X, Guo Z, Zheng R & Xu B. Nitrilotriacetic acid-modified magnetic nanoparticles as a general agent to bind histidine-tagged proteins. *Journal of the American Chemical Society*, *126*(11), 2004, 3392–3393.
12. Fu CM, Wang YF, Guo YF, Lin TY & Chiu JS. In vivo bio-distribution of intravenously injected Tc-99 m labeled ferrite nanoparticles bounded with biocompatible medicals. *IEEE transactions on magnetics*, *41*(10), 2005, 4120–4122.
13. Safarik I & Safarikova M. Use of magnetic techniques for the isolation of cells. *Journal of Chromatography B: Biomedical Sciences and Applications*, *722* (1–2), 1999, 33–53.
14. Sode K, Kudo S, Sakaguchi T, Nakamura N & Matsunaga T. Application of bacterial magnetic particles for highly selective mRNA recovery system. *Biotechnology techniques*, *7*(9), 1993, 688–694.
15. Murthy SR. Low temperature sintering of Ni–Cu–Zn ferrite and its electrical, magnetic and elastic properties. *Journal of Materials Science Letters*, *21*(8), 2002, 657–660.
16. Pardavi-Horvath M. Microwave applications of soft ferrites. *Journal of Magnetism and Magnetic Materials*, *215*, 2000,171–183.
17. Waldron RD. Infrared spectra of ferrites. *Physical review*, *99*(6), 1955, 1727.
18. Gorter EW. Saturation magnetization and crystal chemistry of ferrimagnetic oxides. I. II. Theory of ferrimagnetism. *Philips Res. Rep.*, *9*, 1954, 295–320.
19. Modi KB, Shah SJ, Pujara NB, Pathak TK., Vasoya NH & Jhala IG. Infrared spectral evolution, elastic, optical and thermodynamic properties study on mechanically milled $Ni_{0.5}Zn_{0.5}Fe_2O_4$ spinel ferrite. *Journal of Molecular Structure*, *1049*,2013, 250–262.
20. Patange SM, Shirsath SE, Jadhav SP, Hogade VS, Kamble SR & Jadhav KM. Elastic properties of nanocrystalline aluminum substituted nickel ferrites prepared by co-precipitation method. *Journal of Molecular Structure*, *1038*,2013, 40–44.
21. Pathak TK, Buch JJU, Trivedi UN, Joshi HH & Modi KB. Infrared spectroscopy and elastic properties of nanocrystalline Mg–Mn ferrites prepared by co-precipitation technique. *Journal of nanoscience and nanotechnology*, *8*(8),2008,4181–4187.
22. Modi KB, Gajera JD, Pandya MP, Vora G & Joshi HH. Far-infrared spectral studies of magnesium and aluminum co-substituted lithium ferrites. *Pramana*, *62*(5), 2004, 1173-1180.
23. Bhatu S S, Lakhani VK, Tanna AR, Vasoya NH, Buch JU, Sharma PU & Modi KB. Effect of nickel substitution on structural, infrared and elastic properties of lithium ferrite. *Ind. J. Pure Appl. Phys.* 4, 2007,:596.
24. Patil VG, Shirsath SE, More SD, Shukla SJ & Jadhav KM Effect of zinc substitution on structural and elastic properties of cobalt ferrite. *Journal of Alloys and Compounds*, *488*(1),2009, 199–203.